Supplementary Information

Bending-induced enhanced spatial separation of dopants and long-lived conventional nanoribbon p-n junctions

Xu Liu, [a] Yu-Run Yang, [a] Jing Wang, [a] Rui-Ping Xu, [a] Zhao Liu *[ab] and Ying Liu [ac]

[a] Department of Physics and Hebei Advanced Thin Film Laboratory, Hebei Normal University, Shijiazhuang 050024, China

[b] Beijing Computational Science Research Center, Beijing, 100193, China

[c] National Key Laboratory for Materials Simulation and Design, Beijing, 100083, China

* Authors to whom correspondence should be addressed: zliu@hebtu.edu.cn

S1. Computational parameters.

In generalized Bloch theorem coupled with the self-consistent charge density-functional tight-binding (SCC-DFTB) calculation, the inputs include: (i) file with the suffix ".gen", containing geometry structure with the specific bending angle. (ii) files with the suffix ".skf", containing elemental on-site energies, hopping, overlap, and pair potential parameters between elements, which have been included in various parameter sets and can be downloaded from the DFTB website [1-4]. In this work, we used the 3ob-3-1, matsci-0-3, hyb-0-2, halorg-0-1, and znorg-0-1 parameter sets. Some .skf files (Si-B.skf, B-Si.skf, Si-Ge.skf, Ge-Si.skf, H-Ge.skf, Ge-H.skf, Ge-Ge.skf, Zn-Te.skf, Te-Zn.skf, Te-Te.skf, O-Te.skf, and Te-O.skf) are obtained with the help of Prof. Dong-Bo Zhang and Prof. Thomas Frauenheim (one of the developers of SCC-DFTB method and DFTB+ code). These files are not open and can be available by contacting us. The parameter sets are listed in Table S1 and they all have been checked in previous works. With (i) and (ii), the results in our study can be reproduced and will not be influenced by any other parameters.

Note: The DFTB method was first developed by Gotthard Seifert (G. Seifert, H. Eschrig and W. Bieger, *Z. Phys. Chem.*, 1986, **267**, 529). Based on this work, Thomas Frauenheim et al. developed SCC-DFTB method.

Table S1. The computational parameters in this work.

| Parameter set	Parameters in the set				
3ob-3-1	Zn-F.skf	F-Zn.skf	O-F.skf	F-O.skf	F-F.skf
	Zn-P.skf	P-Zn.skf	O-P.skf	P-O.skf	P-P.skf
	Zn-C.skf	C-Zn.skf			
matsci-0-3	C-C.skf	H-H.skf	N-N.skf	O-O.skf	Si-Si.skf
	Al-Al.skf	C-H.skf	H-C.skf	C-N.skf	N-C.skf
	H-N.skf	N-H.skf	C-O.skf	O-C.skf	H-O.skf
	O-H.skf	C-Si.skf	Si-C.skf	H-Si.skf	Si-H.skf
	C-Al.skf	Al-C.skf	H-Al.skf	Al-H.skf	C-B.skf
	B-C.skf	B-O.skf	O-B.skf	O-N.skf	N-O.skf
	B-H.skf	H-B.skf	Si-Al.skf	Al-Si.skf	Si-O.skf
	O-Si.skf	Si-N.skf	N-Si.skf	B-B.skf	B-N.skf
	N-B.skf				
hyb-0-2	Ga-Ga.skf	Ga-C.skf	C-Ga.skf	Si-Ga.skf	Ga-Si.skf
	Ga-H.skf	H-Ga.skf	Si-As.skf	As-Si.skf	As-H.skf
	H-As.skf	As-As.skf			
halorg-0-1	C-Br.skf	Br-C.skf	Br-Br.skf	Br-H.skf	H-Br.skf
znorg-0-1	Zn-Zn.skf	Zn-O.skf	O-Zn.skf		
	Si-B.skf [a]	B-Si.skf [a]	Si-Ge.skf [a]	Ge-Si.skf [a]	H-Ge.skf [a]
	Ge-H.skf [a]	Ge-Ge.skf [a]	Zn-Te.skf [a]	Te-Zn.skf [a]	Te-Te.skf [a]
	O-Te.skf [a]	Te-O.skf [a]			

[a] Available by contacting authors

Additionally, to minimize the dopants interaction, we select 1×1×3 supercells as primitive motif for armchair NRs, and 1×1×6 supercells as primitive motif for zigzag NRs.

References

1. B. Hourahine, B. Aradi, V. Blum, F. Bonafé, A. Buccheri, C. Camacho, C. Cevallos, M. Y. Deshaye, T. Dumitrică, A. Dominguez, S. Ehlert, M. Elstner, T. van der Heide, J. Hermann, S. Irle, J. J. Kranz, C. Köhler, T. Kowalczyk, T. Kubař, I. S. Lee, V. Lutsker, R. J. Maurer, S. K. Min, I. Mitchell, C. Negre, T. A. Niehaus, A. M. N. Niklasson, A. J. Page, A. Pecchia, G. Penazzi, M. P. Persson, J. Řezáč, C. G. Sánchez, M. Sternberg, M. Stöhr, F. Stuckenberg, A. Tkatchenko, V. W.-Z. Yu and T. Frauenheim, *J. Chem. Phys.*, 2020, **152**, 124101.

2. M. Elstner, D. Porezag, G. Jungnickel, J. Elsner, M. Haugk, T. Frauenheim, S. Suhai and G. Seifert, *Phys. Rev. B*, 1998, **58**, 7260-7268.

3. D. Porezag, T. Frauenheim, T. Köhler, G. Seifert and R. Kaschner, *Phys. Rev. B*, 1995, **51**, 12947-12957.

4. DFTB parameters website, https://dftb.org/parameters; DFTB+ code website, https://dftbplus.org.
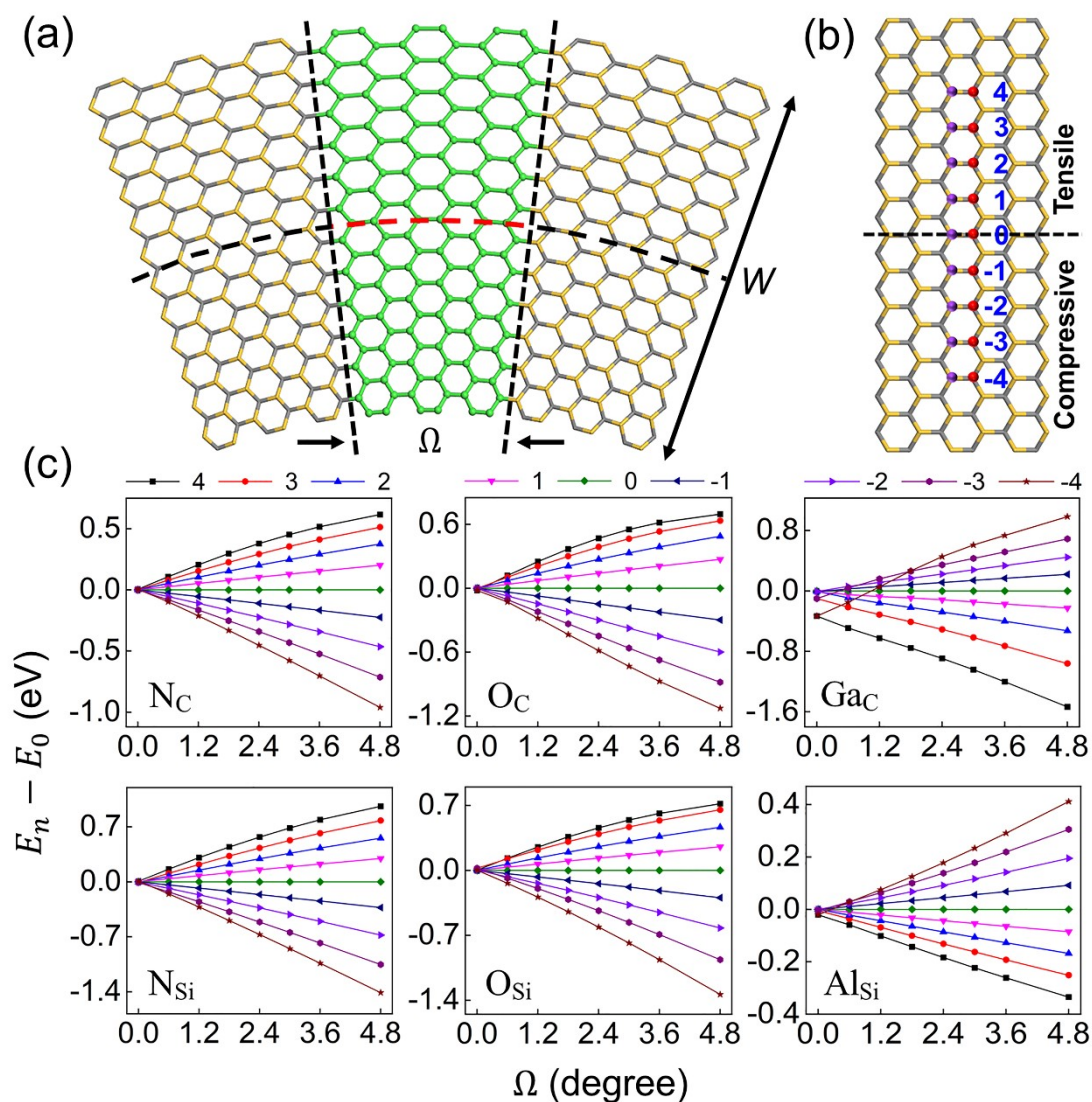
S2. Relative formation energy versus bending angle (armchair SiNR).
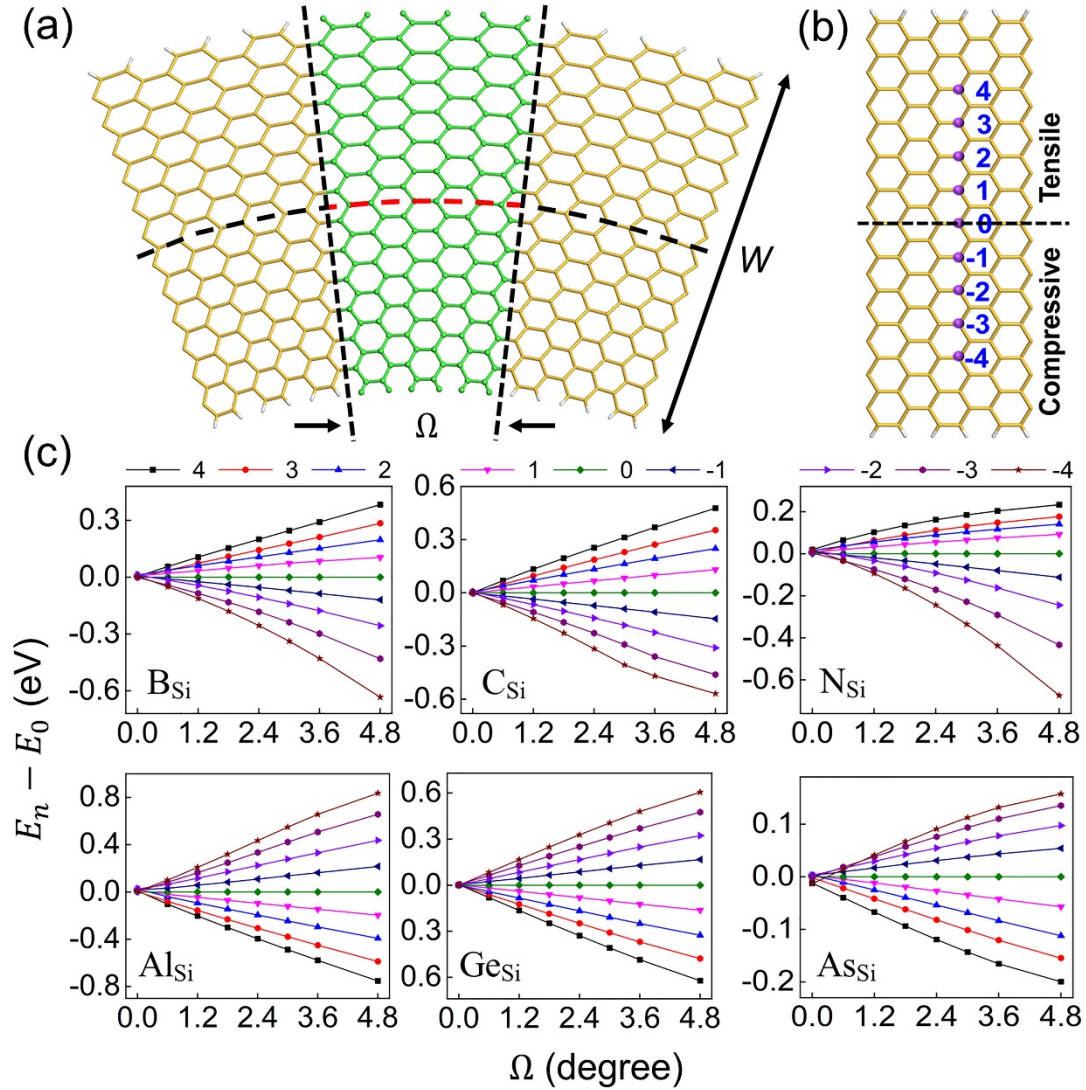
Fig. S1 (a) A 4.6 nm-wide armchair SiNR with a bending angle Ω. The primitive motif in calculation is in green color, and the dashed arc indicates the strain-free line. Si atoms are colored in yellow, and H atoms in white. The red dashed arc represents the length of translation vector of the strain-free NR. (b) 9 doping sites (purple balls) along the radial direction: sites $n = 1, 2, 3, 4$ are on the tensile side, sites $n = -4, -3, -2, -1$ are on the compressive side, and site $n = 0$ is on the strain-free line. (c) The relative formation energy $E_n - E_0$ at site n versus bending angle Ω for various doping cases,

denoted as X_{Si} (X = B, C, N, Al, Ge, As), where the host Si atom is substituted with the dopant X atom.

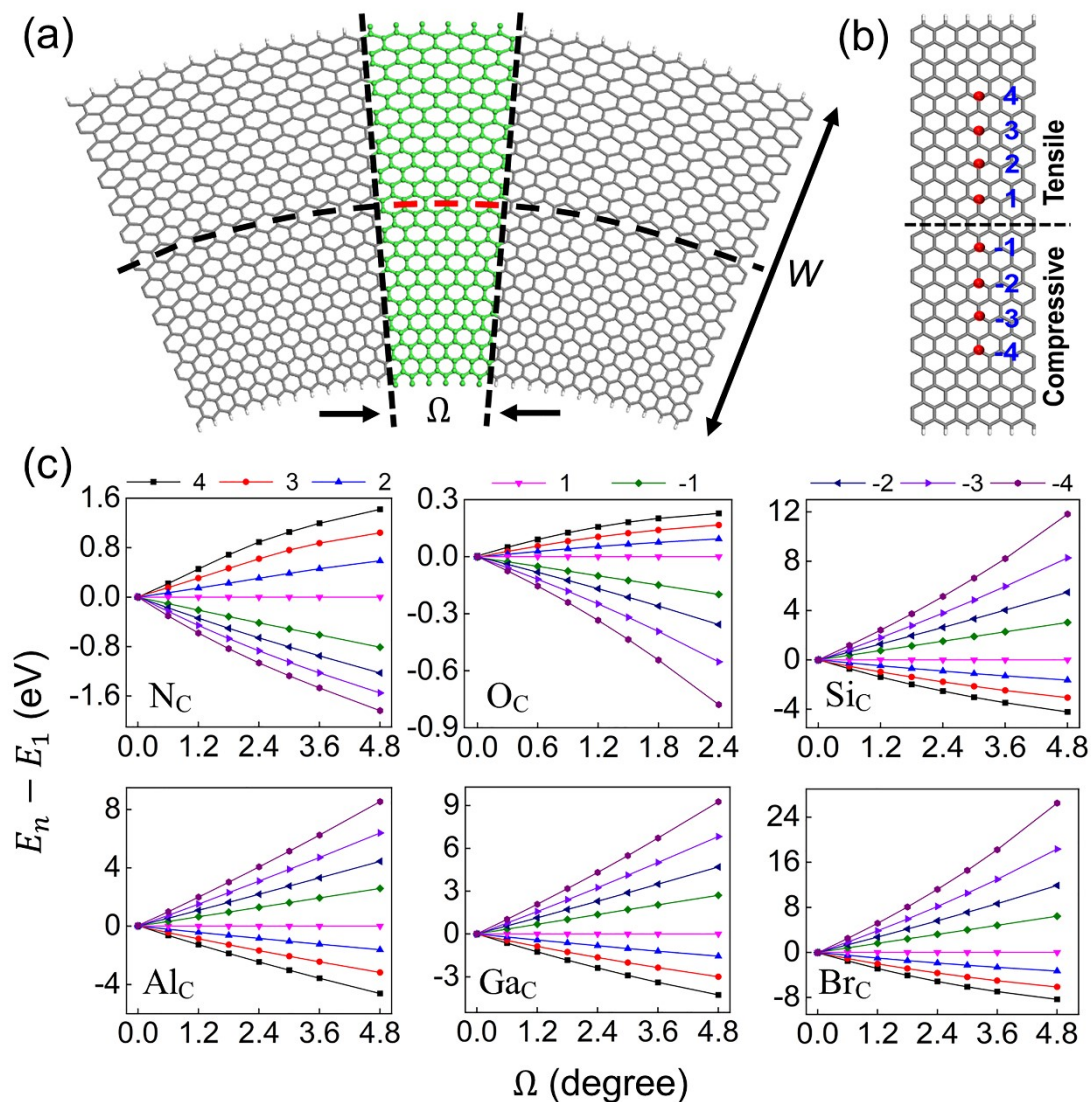**S3. Relative formation energy versus bending angle (armchair SiCNR).**

Fig. S2 (a) A 3.7 nm-wide armchair SiCNR with a bending angle Ω. The primitive

motif in calculation is in green color, and the dashed arc indicates the strain-free line.

The Si and C atoms are depicted in yellow and gray colors, respectively. The red dashed

arc represents the length of translation vector of the strain-free NR. (b) 9 doping sites

along the radial direction (Si sites: purple balls; C sites: red balls): sites $n = 1, 2, 3, 4$

are on the tensile side, sites $n = -4, -3, -2, -1$ are on the compressive side, and site

$n = 0$ is on the strain-free line. (c) The relative formation energy $E_n - E_0$ at site n versus

bending angle Ω for various doping cases, denoted as X_C (X = N, O, Ga) and Y_{Si} (Y = N, O, Al), where the host C and Si atoms are substituted with the dopant X and Y atoms, respectively.
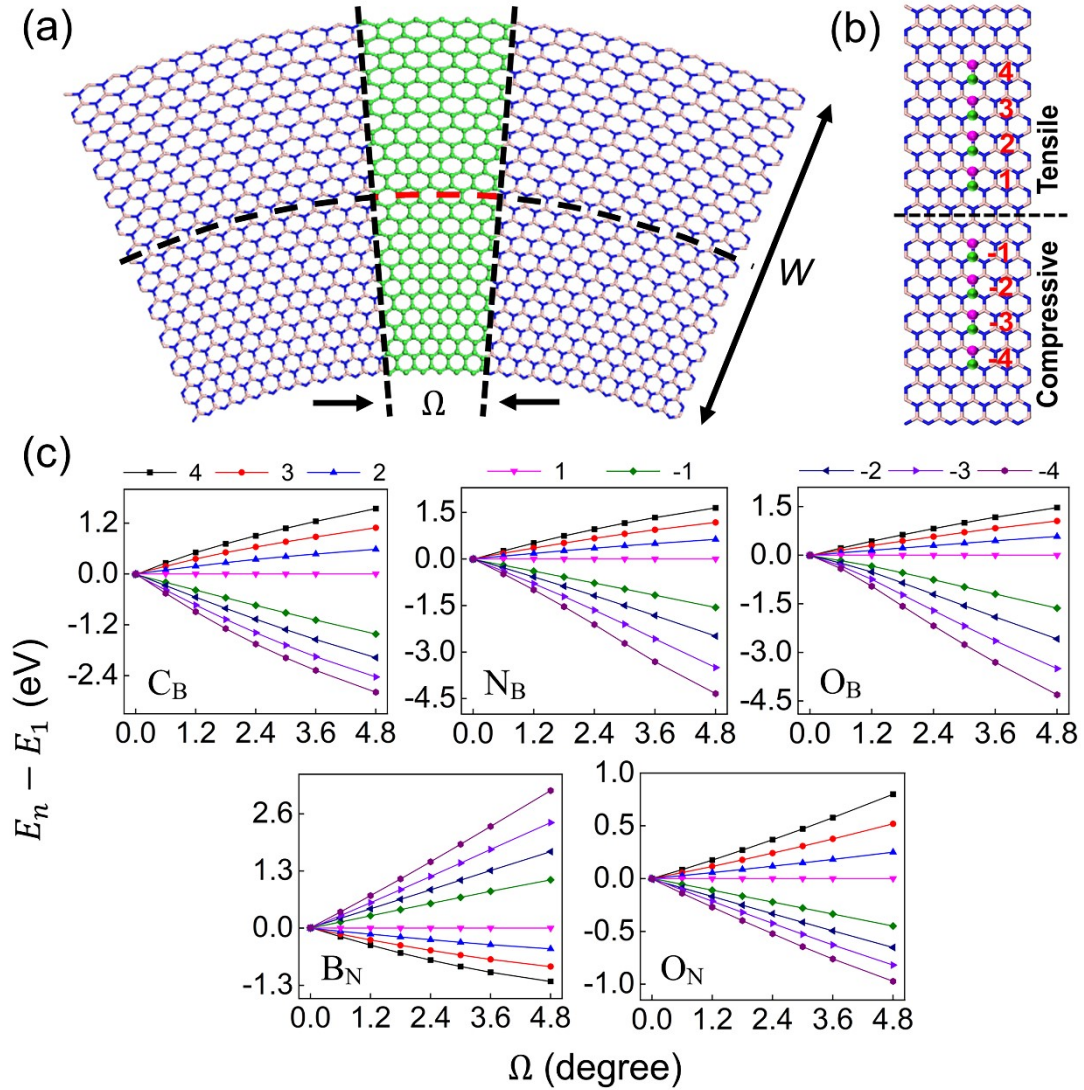
S4. Relative formation energy versus bending angle (zigzag GNR).

Fig. S3 (a) A 5.0 nm-wide zigzag GNR with a bending angle Ω. The primitive motif in calculation is in green color, and the dashed arc indicates the strain-free line. C atoms are colored in gray, and H atoms in white. The red dashed arc represents the length of translation vector of the strain-free NR. (b) 8 doping sites (red balls) along the radial direction: sites $n = 1, 2, 3, 4$ are on the tensile side, sites $n = -4, -3, -2, -1$ are on the compressive side. (c) The relative formation energy $E_n - E_1$ at site n versus bending

angle Ω for various doping cases, denoted as X_C (X = N, O, Si, Al, Ga, Br), where the

host C atom is substituted with the dopant X atom.

S5. Relative formation energy versus bending angle (zigzag BNNR).

Fig. S4 (a) A 5.1 nm-wide zigzag BNNR with a bending angle Ω. The primitive motif in calculation is in green color, and the dashed arc indicates the strain-free line. The B and N atoms are depicted in pink and blue colors, respectively. The red dashed arc represents the length of translation vector of the strain-free NR. (b) 8 doping sites along the radial direction (B sites: green balls; N sites: rose balls): sites $n = 1, 2, 3, 4$ are on the tensile side, sites $n = -4, -3, -2, -1$ are on the compressive side. (c) The relative formation energy $E_n - E_1$ at site n versus bending angle Ω for various doping cases,

denoted as X_N (X = B, O) and Y_B (Y = C, N, O), where the host N and B atoms are

substituted with the dopant X and Y atoms, respectively.

S6. Relative formation energy versus bending angle (zigzag ZnONR).
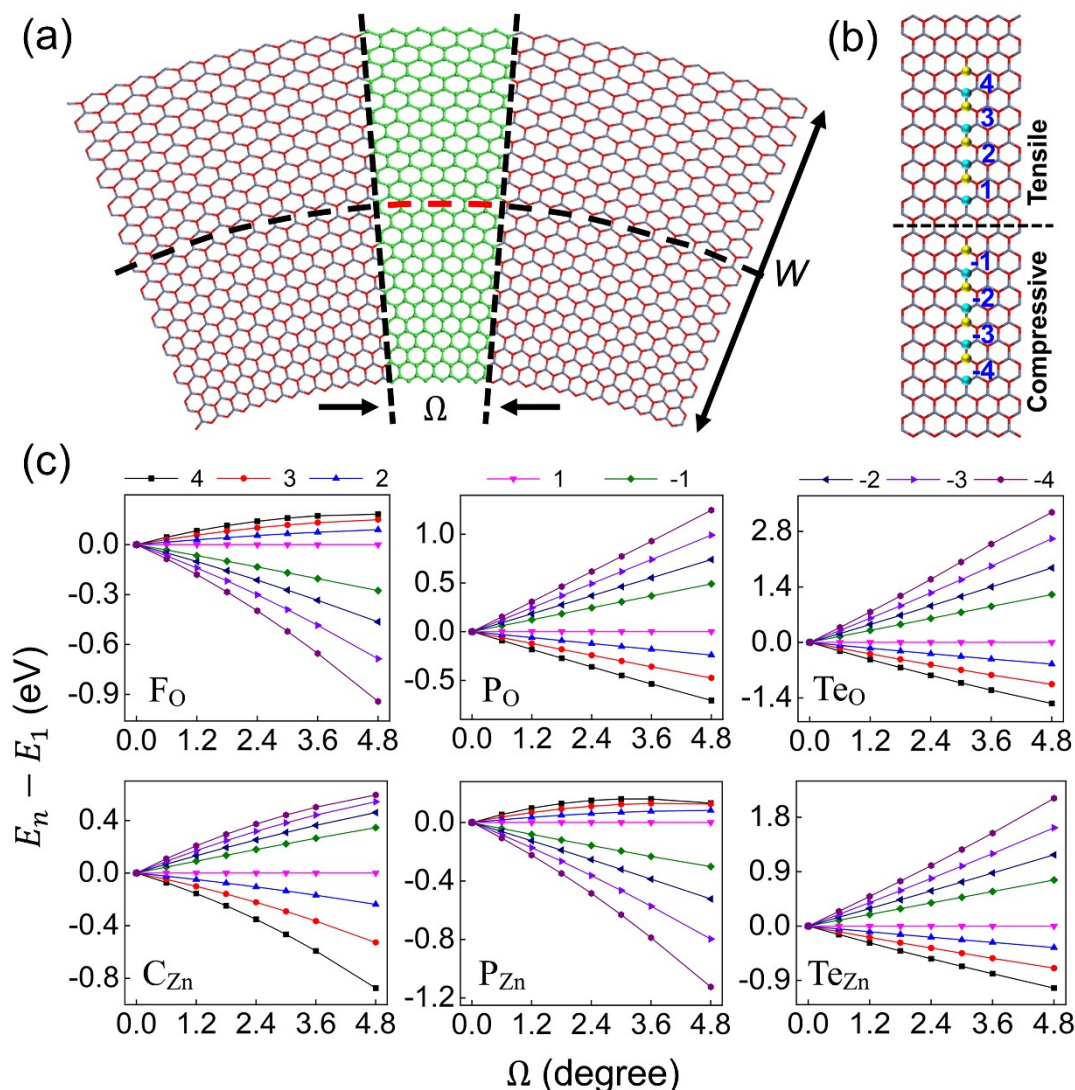
Fig. S5 (a) A 6.6 nm-wide zigzag ZnONR with a bending angle Ω. The primitive motif in calculation is in green color, and the dashed arc indicates the strain-free line. The Zn and O atoms are depicted in silver and red colors, respectively. The red dashed arc represents the length of translation vector of the strain-free NR. (b) 8 doping sites along the radial direction (Zn sites: yellow balls; O sites: blue balls): sites $n = 1, 2, 3, 4$ are on the tensile side, sites $n = -4, -3, -2, -1$ are on the compressive side. (c) The relative formation energy $E_n - E_1$ at site n versus bending angle Ω for various doping

cases, denoted as X_O (X = F, P, Te) and Y_{Zn} (Y = C, P, Te), where the host O and Zn

atoms are substituted with the dopant X and Y atoms, respectively.

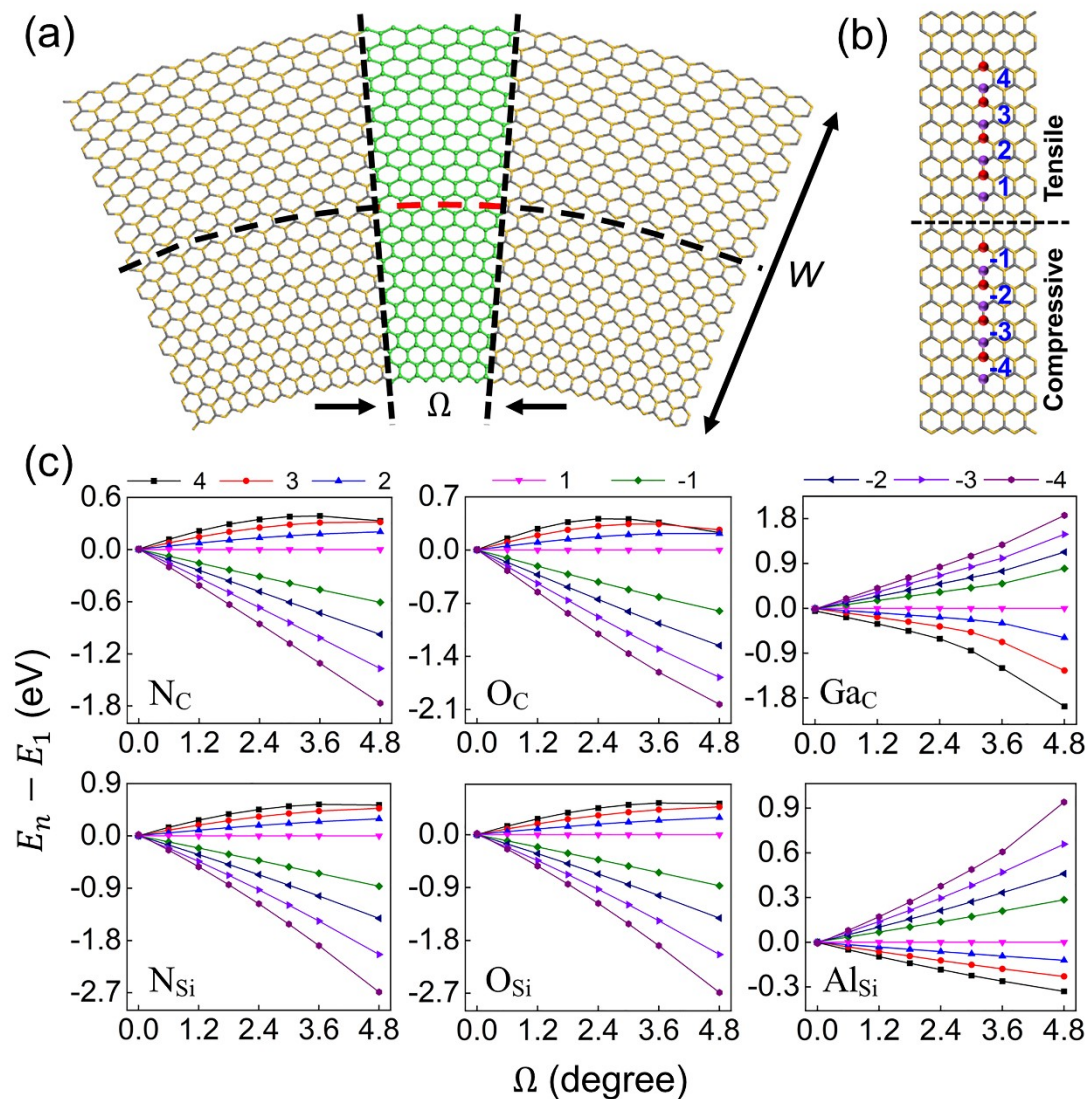**S7. Relative formation energy versus bending angle (zigzag SiNR).**
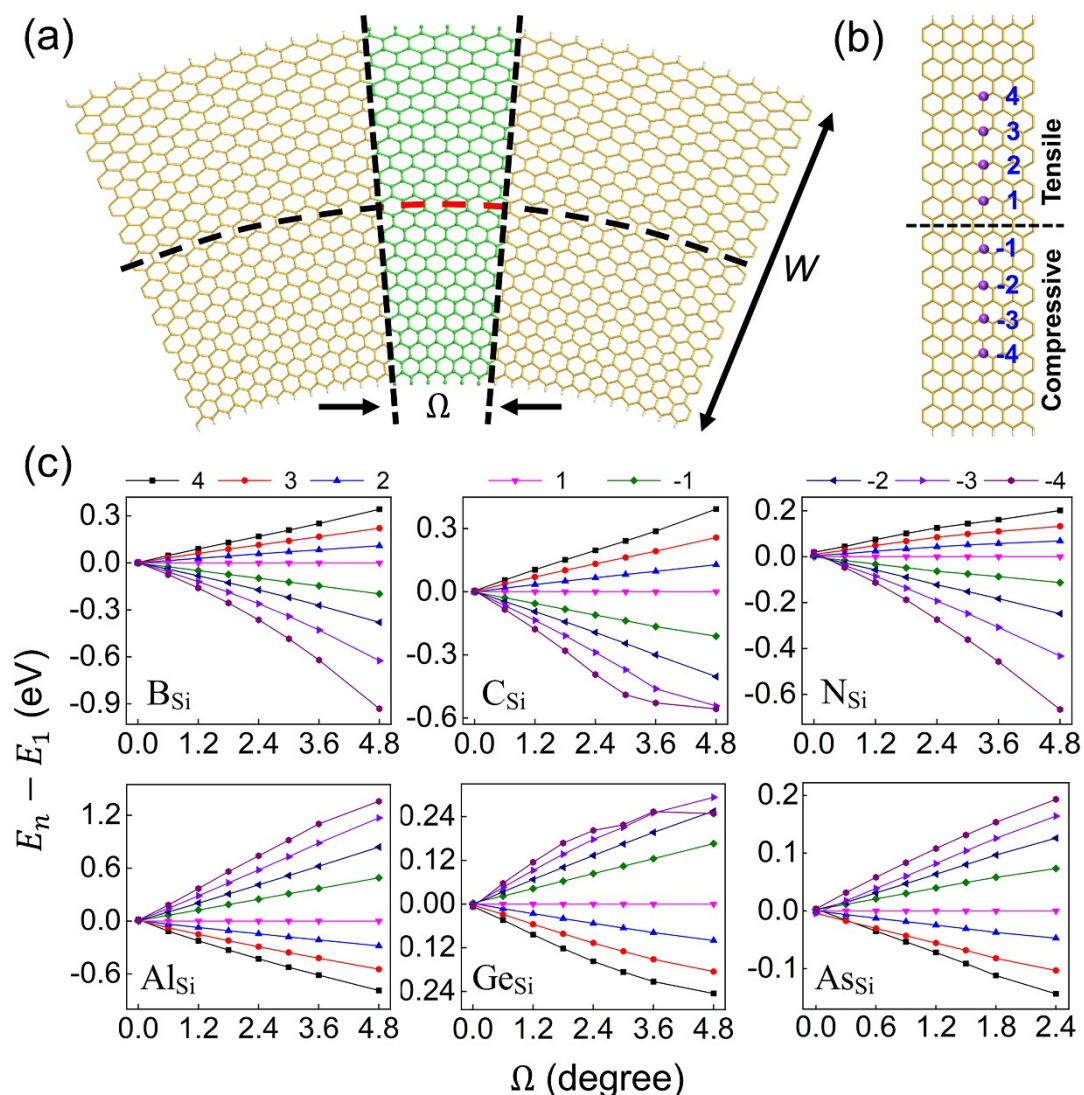
Fig. S6 (a) A 7.8 nm-wide zigzag SiNR with a bending angle Ω. The primitive motif in

calculation is in green color, and the dashed arc indicates the strain-free line. Si atoms

are colored in yellow, and H atoms in white. The red dashed arc represents the length

of translation vector of the strain-free NR. (b) 8 doping sites (purple balls) along the

radial direction: sites $n = 1, 2, 3, 4$ are on the tensile side, sites $n = -4, -3, -2, -1$

are on the compressive side. (c) The relative formation energy $E_n - E_1$ at site n versus

bending angle Ω for various doping cases, denoted as X_{Si} (X = B, C, N, Al, Ge, As),

where the host Si atom is substituted with the dopant X atom.

S8. Relative formation energy versus bending angle (zigzag SiCNR).

Fig. S7 (a) A 6.2 nm-wide zigzag SiCNR with a bending angle Ω. The primitive motif in calculation is in green color, and the dashed arc indicates the strain-free line. The Si and C atoms are depicted in yellow and gray colors, respectively. The red dashed arc represents the length of translation vector of the strain-free NR. (b) 8 doping sites along the radial direction (Si sites: purple balls; C sites: red balls): sites $n = 1, 2, 3, 4$ are on the tensile side, sites $n = -4, -3, -2, -1$ are on the compressive side. (c) The relative formation energy $E_n - E_1$ at site n versus bending angle Ω for various doping cases,

denoted as X_C (X = N, O, Ga) and Y_{Si} (Y = N, O, Al), where the host C and Si atoms

are substituted with the dopant X and Y atoms, respectively.

S9. The relative formation energy $E_{n_1,n_2} - E_{1,-1}$ **of co-doped zigzag NRs, with two dopants at site** n_1 **and site** n_2.
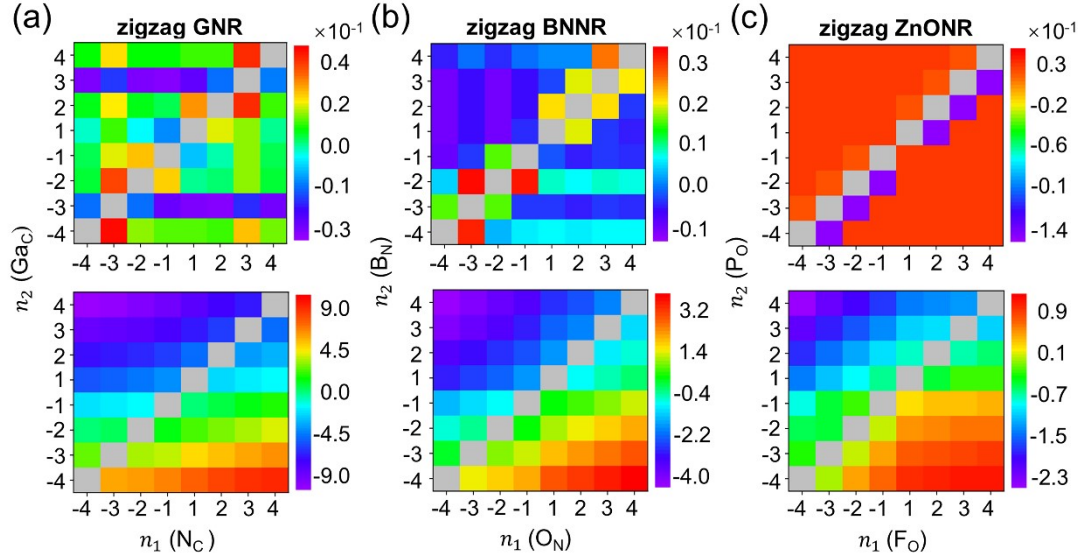
Fig. S8 The relative formation energy $E_{n_1,n_2} - E_{1,-1}$ of co-doped zigzag NRs, with two dopants at site n_1 and site n_2. The NRs and doping sites are the same as those in Figs. S3-S7. The grey-colored region represents the impossibility of co-doping on the same doping site. (a) GNR with bending angles $\Omega = 0$ (upper panel) and $\Omega = 4.8°$ (lower panel), co-doped with N and Ga atoms; (b) BNNR with bending angles $\Omega = 0$ (upper panel) and $\Omega = 4.8°$ (lower panel), co-doped with O and B atoms, both at N sites; (c) ZnONR, with bending angles $\Omega = 0$ (upper panel) and $\Omega = 4.8°$ (lower panel), co-doped with F and P atoms, both at O sites.

S10. Certain structural information.

Table S2. Relaxed structures that cannot meet the convergence tolerances (charge: 10^{-6} e; force: 10^{-6} eV Å^{-1}).

Structure and doping site	Ω (°)	Charge convergence (e)	Force convergence (eV Å^{-1})
A-GNR-O_C $n = 4$[a]	0.0	10^{-4}	10^{-4}
A-GNR-O_C $n = 4$	0.6	10^{-5}	10^{-4}
A-GNR-O_C $n = 3$	0.0	10^{-4}	10^{-4}
A-GNR-O_C $n = 3$	0.6	10^{-5}	10^{-4}
A-GNR-O_C $n = 2$	0.0	10^{-4}	10^{-4}
A-GNR-O_C $n = 2$	0.6	10^{-5}	10^{-5}
A-GNR-O_C $n = 2$	1.2	10^{-5}	10^{-5}
A-GNR-O_C $n = 1$	0.0	10^{-4}	10^{-4}
A-GNR-O_C $n = 1$	0.6	10^{-5}	10^{-5}
A-GNR-O_C $n = -1$	0.0	10^{-4}	10^{-4}
A-GNR-O_C $n = -2$	0.0	10^{-4}	10^{-4}
A-GNR-O_C $n = -2$	0.6	10^{-5}	10^{-4}
A-GNR-O_C $n = -2$	1.2	10^{-5}	10^{-5}
A-GNR-O_C $n = -3$	0.0	10^{-5}	10^{-4}
A-GNR-O_C $n = -4$	0.0	10^{-5}	10^{-4}
A-BNNR-O_B $n = -4$	-4.8	10^{-5}	10^{-5}
A-SiNR-As_{Si} $n = 4$	0.0	10^{-5}	10^{-4}
A-SiNR-As_{Si} $n = -4$	0.0	10^{-4}	10^{-4}
A-SiNR-As_{Si} $n = -4$	0.6	10^{-5}	10^{-5}
A-SiCNR-Ga_C $n = 4$	0.0	10^{-4}	10^{-4}
A-SiCNR-Ga_C $n = 4$	0.6	10^{-4}	10^{-4}
A-SiCNR-Ga_C $n = 4$	1.2	10^{-5}	10^{-4}
A-SiCNR-Ga_C $n = 3$	0.0	10^{-5}	10^{-4}
A-SiCNR-Ga_C $n = 2$	0.6	10^{-5}	10^{-5}
A-SiCNR-Ga_C $n = -3$	0.0	10^{-4}	10^{-4}
A-SiCNR-Ga_C $n = -3$	0.6	10^{-5}	10^{-4}
A-SiCNR-Ga_C $n = -4$	0.0	10^{-4}	10^{-4}

Structure and doping site	Ω ($^\circ$)	Charge convergence (e)	Force convergence (eV Å^{-1})
A-SiCNR-Ga$_C$ $n = -4$	0.6	10^{-4}	10^{-4}
A-SiCNR-Ga$_C$ $n = -4$	1.2	10^{-4}	10^{-4}
A-SiCNR-Ga$_C$ $n = -4$	1.8	10^{-5}	10^{-4}
Z-ZnONR-P$_{Zn}$ $n = 4$	4.8	10^{-5}	10^{-5}
Z-SiNR-C$_{Si}$ $n = -3$	4.8	10^{-5}	10^{-5}
Z-SiNR-C$_{Si}$ $n = -4$	4.8	10^{-5}	10^{-4}
Z-SiNR-Ge$_{Si}$ $n = -4$	3.0	10^{-4}	10^{-4}
Z-SiNR-Ge$_{Si}$ $n = -4$	3.6	10^{-4}	10^{-4}
Z-SiNR-Ge$_{Si}$ $n = -4$	4.8	10^{-4}	10^{-4}
Z-SiNR-As$_{Si}$ $n = 4$	0.0	10^{-4}	10^{-4}
Z-SiNR-As$_{Si}$ $n = 4$	0.3	10^{-4}	10^{-4}
Z-SiNR-As$_{Si}$ $n = -3$	0.0	10^{-4}	10^{-4}
Z-SiNR-As$_{Si}$ $n = -3$	0.3	10^{-5}	10^{-5}
Z-SiCNR-N$_C$ $n = 4$	4.8	10^{-5}	10^{-5}
Z-SiCNR-O$_C$ $n = 4$	3.6	10^{-5}	10^{-4}
Z-SiCNR-O$_C$ $n = 4$	4.8	10^{-4}	10^{-4}
Z-SiCNR-Ga$_C$ $n = 4$	4.8	10^{-5}	10^{-5}
Z-SiCNR-N$_{Si}$ $n = 4$	4.8	10^{-6}	10^{-5}
Z-SiCNR-O$_{Si}$ $n = 4$	4.8	10^{-5}	10^{-5}
Z-SiCNR-Al$_{Si}$ $n = 4$	4.8	10^{-6}	10^{-5}

[a] "A-GNR" denotes armchair GNR; "O$_C$" represents that O element substitutes C element; $n = 4$ represents the dopant atom at the doping site $n = 4$.